Supporting information

Slow Magnetic Relaxation in High-Coordinate Co(II) and Fe(II) Compounds bearing Neutral Tetradentate Ligands

Min Peng,[a†] Xiao-Fan Wu,[b†] Li-Xin Wang,[a] Si-Huai Chen,[c] Jing Xiang,*[a] Xin-Xin Jin,[b] Shek-Man Yiu,[e] Bing-Wu Wang,*[b] Song Gao,*[b,d] Tai-Chu Lau*[e]

[a] College of Chemistry and Environmental Engineering, Yangtze University, Jingzhou 434020, HuBei, P. R. China

[b] State Key Laboratory of Rare Earth Materials Chemistry and Applications and PKU-HKU Joint Laboratory on Rare Earth Materials and Bioinorganic Chemistry, Peking University, Beijing 100871, P. R. China

[c] School of Chemistry and Environmental Engineering, Wuhan Institute of Technology, Wuhan 430073, P. R. China

[d] South China University of Technology, P. R. China

[e] Department of Chemistry, City University of Hong Kong, Tat Chee Avenue, Kowloon Tong, Hong Kong 999077, P. R. China

† these authors contributed equally.

Experimental Section

Materials and physical measurements

IR spectra were obtained as KBr discs using a Nicolet 360 FT-IR spectrophotometer. UV/vis spectra were recorded on a Perkin Elmer Lambda 19 spectrophotometer in 1 cm quartz cuvettes. Elemental analysis was performed using an Elementar Vario EL Analyzer. Cyclic voltammetry (CV) was performed with a CH Instruments Electrochemical Workstation CHI660C. A glassy carbon working electrode, a Pt wire counter electrode, and a saturated calomel electrode (SCE) as reference electrode were used. Variable-temperature magnetic susceptibility, ac magnetic susceptibility, and field dependence of magnetization were measured on a Quantum Design MPMS XL-5 SQUID system using powder samples made from the crystal samples. Background corrections were done by experimental measurement on the sample holder. The experimental susceptibilities were corrected for the diamagnetism of the constituent atoms (Pascal's tables).

X-ray crystallography

Crystals suitable for X-ray diffraction analysis were obtained for **1, 2** and **3**. X-ray diffraction data were collected on SuperNova, Dual, Cu at zero, AtlasS2 diffractometer for **1,** Xcalibur, Sapphire3, Gemini ultra-diffractometer (Agilent, Santa Clara, CA, USA) for **2**, and Bruker D8 Venture Photon II diffractometer for **3** using graphite-monochromated Cu-K_α ($\lambda = 1.54178$ Å) or Mo-K_α ($\lambda = 0.71073$ Å) radiation. The structures were solved by direct methods employing the SHELXL-2016 (Fe, Co) and SHELXL-2018 (Ni) program and refined by full-matrix least-squares using SHELX-2016 on personal computer (PC). All non-hydrogen atoms were refined anisotropically. H atoms were generated by the program SHELXL-2016. The positions of H atoms were calculated based on riding mode with thermal parameters equal to 1.2 times that of the associated C atoms and participated in the calculation of final R-indices. Crystallographic data (excluding structure factors) for the structures in this paper have been deposited with the Cambridge Crystallographic Data Centre, CCDC, 12 Union Road, Cambridge CB21EZ, UK. Copies of the data can be obtained free of charge on quoting the depository numbers CCDC 2041098, 2041099, 2041100 for these compounds.
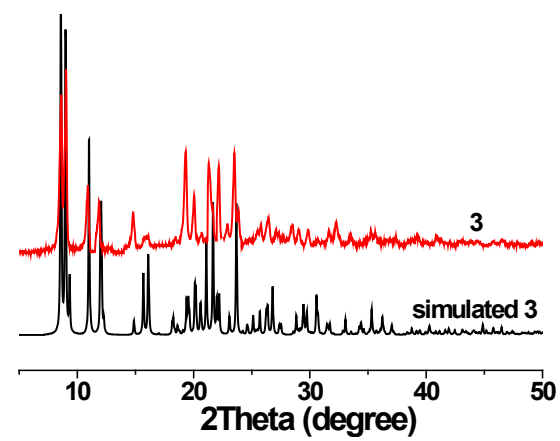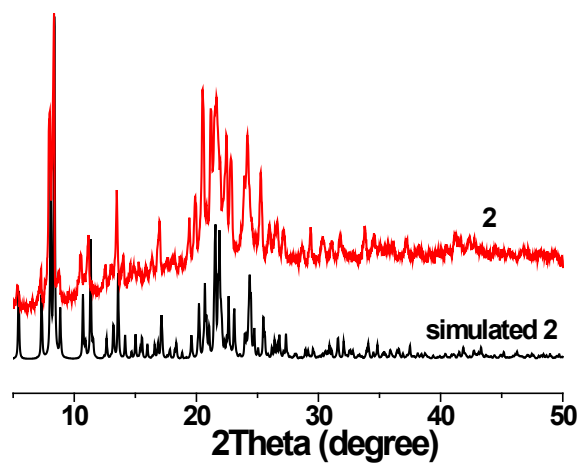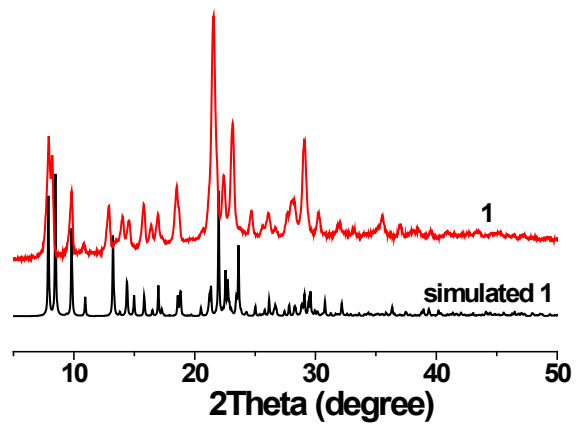
Figure S1. The calculated X-ray powder diffraction patterns (black) and the experimental one (red) of **1, 2** and **3**.
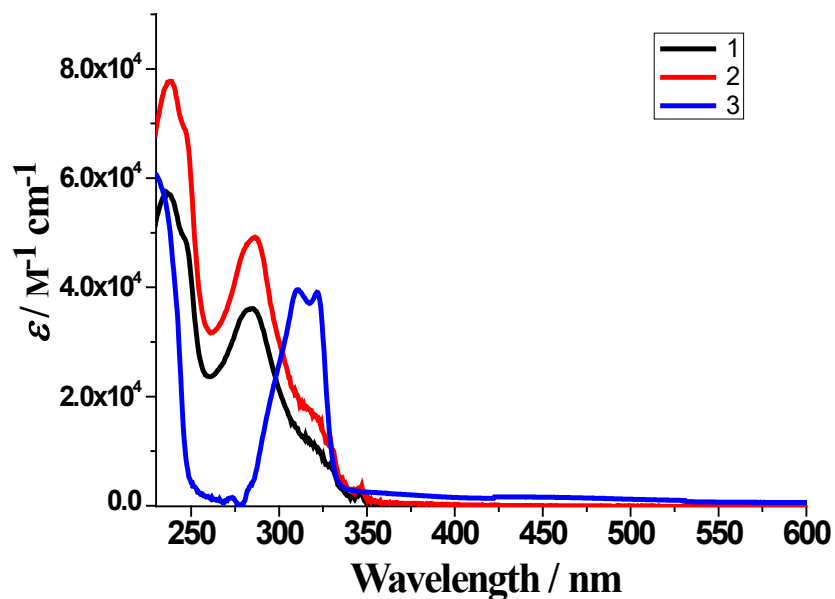
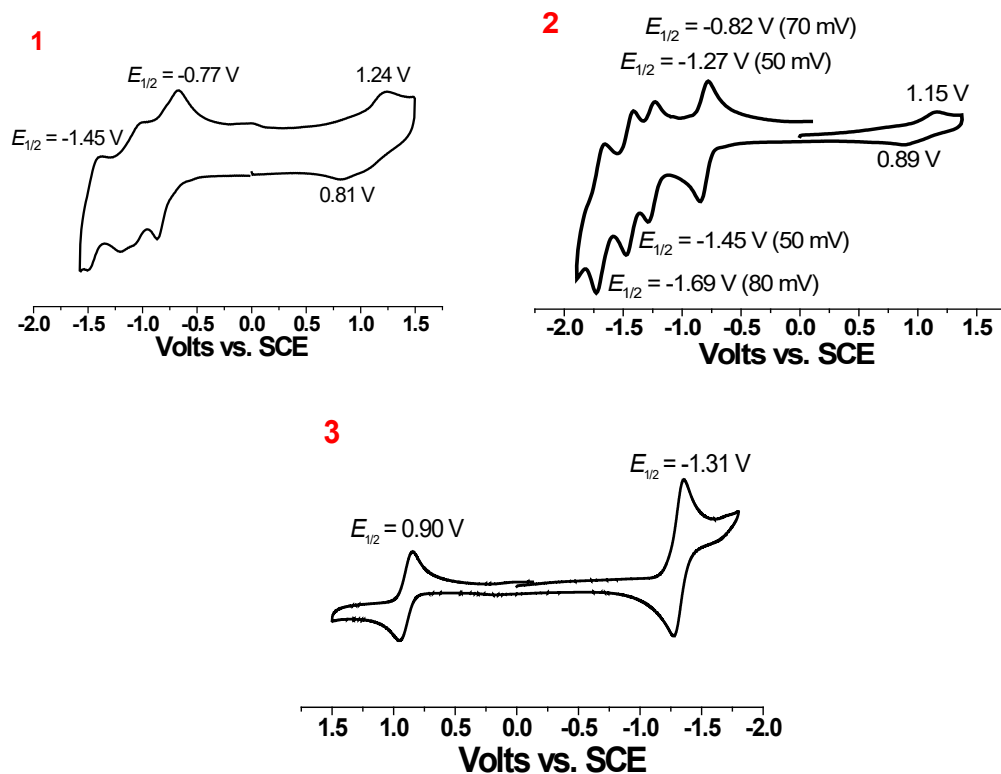**Figure S2.** UV/vis spectra of **1-3** in MeCN.

Figure S3. CV of **1-3** in MeCN containing 0.1 M [^{n}Bu$_4$N]PF$_6$ with scan rate 100 mV·s^{-1}.
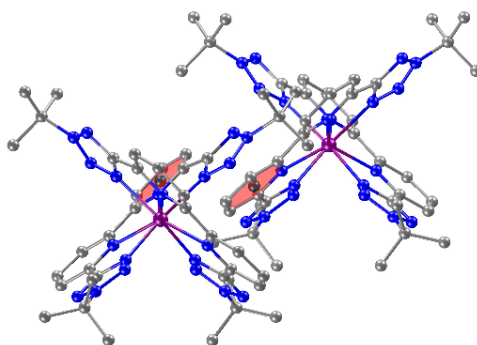
Figure S4. The weak $\pi \cdots \pi$ stacking interactions in **3**.
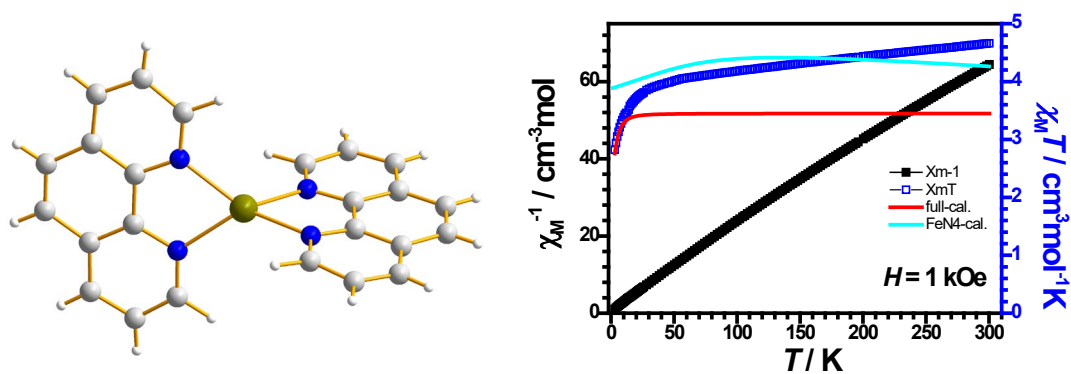
Figure S5. Left: FeN$_4$ core reduced from [Fe(L^4)$_2$](ClO$_4$)$_2$ (**5**) for ab initio calculations; right: χ_MT values for experimental result (blue), full structure calculation (red), reduced FeN$_4$ core calculation (light blue).
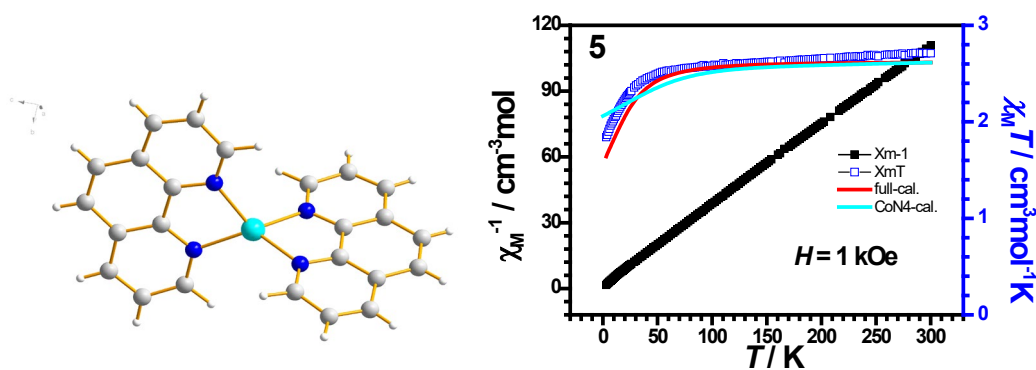
Figure S6. Left: CoN$_4$ core reduced from [Co(L^3)$_2$](ClO$_4$)$_2$ [18] for ab initio calculations; right: χ_MT values for experimental result (blue), full structure calculation (red), reduced CoN$_4$ core calculation (light blue).

Figure S7. Temperature dependence of in-phase (χ') signal of the *ac* magnetic susceptibility for **2** (H_{dc} = 2 kOe and H_{ac} = 3 Oe)

Figure S8. Frequency dependence of in-phase (χ') signal of the *ac* magnetic susceptibility for **2** (H_{dc} = 2 kOe and H_{ac} = 3 Oe).

Figure S9. Cole–Cole plots of **2** at 2–3.5 K (H_{dc} = 2.0 kOe and H_{ac} = 3 Oe).

Figure S10. Temperature dependence of in-phase (χ') signal of the *ac* magnetic susceptibility for **3** (H_{dc} = 3.2 kOe and H_{ac} = 3 Oe).
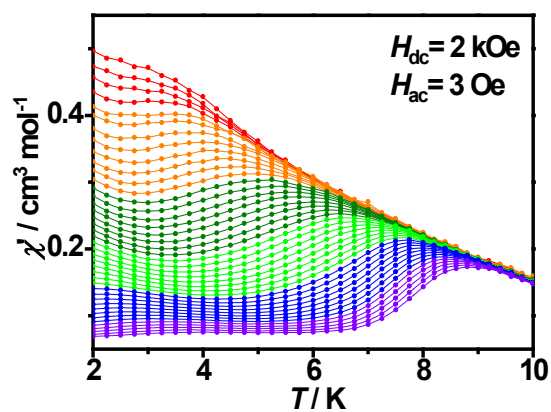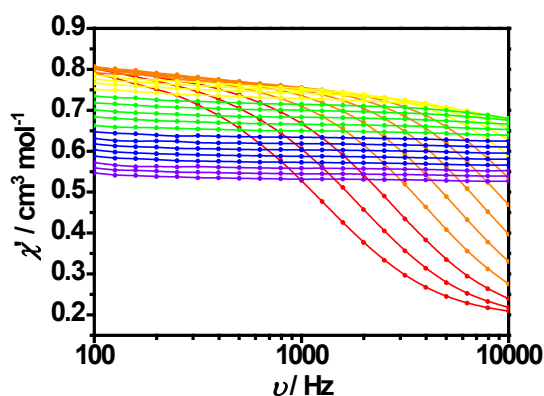

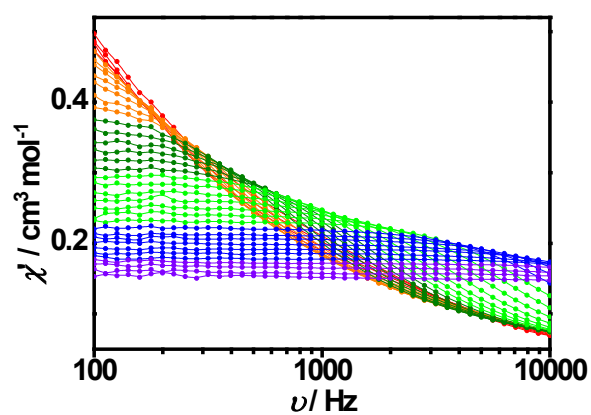**Figure S11.** Frequency dependence of in-phase (χ') signal of the *ac* magnetic susceptibility for **3** (H_{dc} = 3.2 kOe and H_{ac} = 3 Oe).

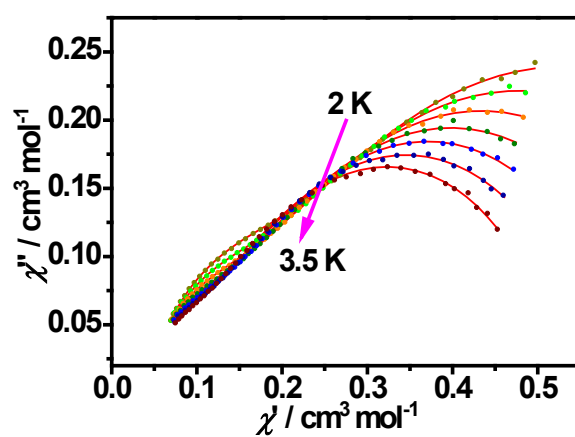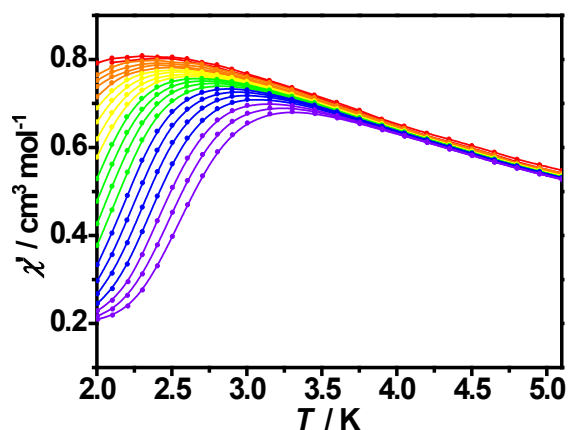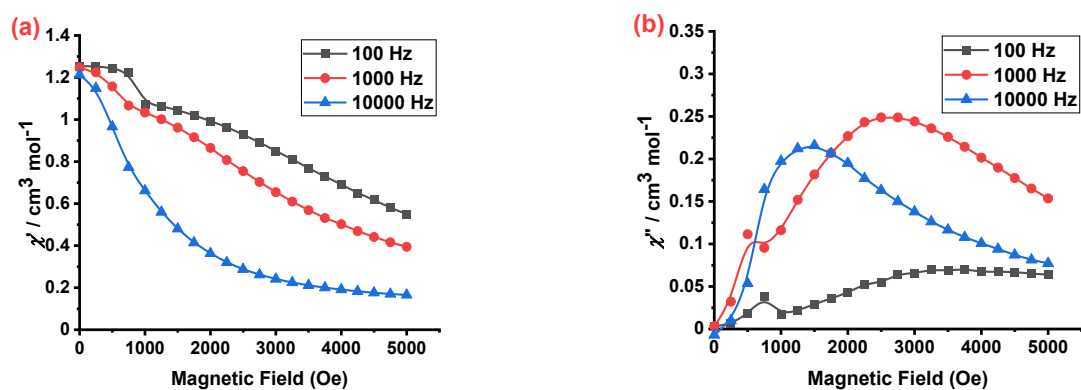
Figure S12. (a) Field dependence of in-phase (χ') signal of the ac magnetic susceptibility for **3** (H_{ac} = 3 Oe); (b) Field dependence of out-of-phase (χ'') signal of the ac magnetic susceptibility for **3** (H_{ac} = 3 Oe).
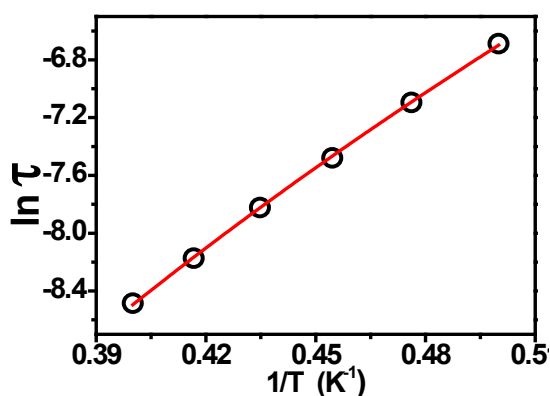
Figure S13. The ln(τ) *vs.* $1/T$ plot for **3** and the red line is fitted by Raman process with equation $\tau^{-1} = CT^{n}$.
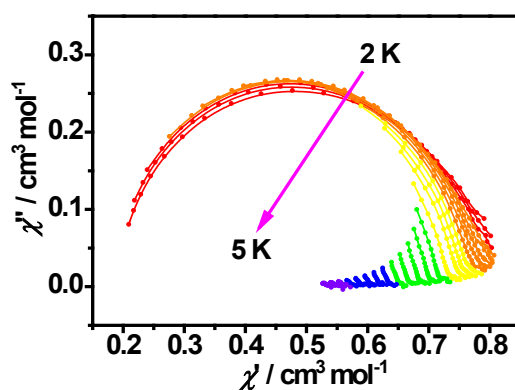
Figure S14. Cole–Cole plots of **3** at 2–5 K (H_{dc} = 3.2 kOe and H_{ac} = 3 Oe).

Table S1. Crystal data and structure refinement details for compounds **1, 2** and **3**.

	1	2	3
Formula	$C_{44}H_{52}N_8NiO_4 \cdot (ClO_4)_2$	$C_{44}H_{52}N_8CoO_4 \cdot (ClO_4)_2$	$C_{40}H_{48}FeN_{20} \cdot (ClO_4)_2 \cdot (CH_3OH)_2$
Mr	1014.54	1014.76	1127.81
T /K	293(2)	173(2)	213(2)
Crystal syst	Monoclinic	Monoclinic	Monoclinic
Space group	Cc	P2(1)/n	P2/n
a/Å	20.9339 (9)	8.7880 (3)	15.9954 (9)
b/Å	13.2633 (6)	24.1051 (6)	10.5941 (5)

c/Å	16.2274 (5)	21.9198 (6)	16.1100 (9)
α, (°)	/	/	/
β, (°)	95.070 (3)	91.512 (2)	92.895 (2)
γ, (°)	/	/	/
V/ Å^3	4488.0 (3)	4641.8 (2)	2726.5 (3)
Z	4	4	2
ρ_{calcd}, Mg m^{-3}	1.502	1.452	1.374
F(000)	2120	2116	1176
Collected refl.	8259	19202	22503
Unique refl.	4985	8934	5606
R(int)	0.025	0.043	0.069
Final R indices,	R_1(obs)= 0.046	R_1(obs)= 0.045	R_1(obs)= 0.057
$I > 2\sigma(I)$	wR(all)= 0.124	wR(all)= 0.115	wR(all)= 0.161
GOF	1.03	1.03	1.02
No.of par.	695	690	422

Table S2. Selected bond orders for **1** and **2**.

	1			**2**	
	Mayer bond orders	Wiberg bond orders		Mayer bond orders	Wiberg bond orders
Ni-N2	0.13862	0.30060	Co-N1	0.11258	0.26358
Ni-N3	0.09497	0.23920	Co-N2	0.11116	0.25182
Ni-N6	0.10432	0.24333	Co-N5	0.11637	0.25962
Ni-N7	0.15737	0.30053	Co-N6	0.10770	0.25914
Ni-O2	0.08675	0.23888	Co-O1	0.14121	0.27501
Ni-O3	/	/	Co-O3	0.12004	0.20792
Ni-O4	0.24432	0.31919	Co-O4	0.11304	0.18791

Table S3. Selected bond orders for **3**.

	3	
	Mayer bond orders	Wiberg bond orders
Fe-N1	0.04572	0.24376
Fe-N5	0.07241	0.19126
Fe-N6	0.06983	0.19290
Fe-N10	0.04689	0.23806

Table S4. Parameters of one-component Debye's model for Co(II) compound **2**.

T / K	χ_S / (cm³ mol⁻¹)	χ_T / (cm³ mol⁻¹)	τ / (s)	α	*Residual*
3.5	0.554926E-01	0.597360E+00	0.565701E-03	0.319866E+00	0.309110E-02
3.75	0.589273E-01	0.539429E+00	0.438003E-03	0.280995E+00	0.287308E-02
4.0	0.601785E-01	0.498182E+00	0.356462E-03	0.253228E+00	0.235435E-02
4.25	0.599451E-01	0.463801E+00	0.295629E-03	0.231631E+00	0.180925E-02
4.5	0.610939E-01	0.430348E+00	0.242865E-03	0.201110E+00	0.171983E-02
4.75	0.602979E-01	0.404648E+00	0.204775E-03	0.182596E+00	0.138082E-02
5.0	0.604759E-01	0.380148E+00	0.171782E-03	0.158014E+00	0.131516E-02
5.25	0.593592E-01	0.361240E+00	0.146006E-03	0.143739E+00	0.956503E-03
5.5	0.587853E-01	0.343845E+00	0.124169E-03	0.126790E+00	0.805198E-03
5.75	0.575795E-01	0.327898E+00	0.105685E-03	0.112681E+00	0.589832E-03
6.0	0.566760E-01	0.313184E+00	0.892492E-04	0.977407E-01	0.483647E-03
6.25	0.554324E-01	0.300611E+00	0.752311E-04	0.856285E-01	0.298254E-03
6.5	0.546844E-01	0.287400E+00	0.627504E-04	0.698981E-01	0.257850E-03
6.75	0.527519E-01	0.273914E+00	0.512467E-04	0.593147E-01	0.169884E-03
7	0.508921E-01	0.263038E+00	0.410295E-04	0.517173E-01	0.209419E-03
7.25	0.494373E-01	0.251153E+00	0.319535E-04	0.370405E-01	0.972400E-04
7.5	0.483912E-01	0.241306E+00	0.247797E-04	0.311291E-01	0.182565E-03

Table S5. Compound **2** and other mononuclear 7-coordinate Co(II) complexes.

Compounds	D/cm⁻¹	E /cm⁻¹	τ_0/s	U_{eff} /cm⁻¹ (K)	ref
[Co(**L¹**)₂](ClO₄)₂	56.2	0.66	3.16×10⁻¹¹	71.4(100)	this work
[Co(H₂dapb)(H₂O)(NO₃)](NO₃)	24.6	-1.4×10⁻²	6.0 ×10⁻¹⁰	56.3(81.2)	8d
[CoL⁹ (H₂O)₂]Cl₂·(H₂O)₄	24.8	1.6×10⁻³	1.2 × 10⁻⁶	20.7(29.8)	8d
[Co(dapb)(im)₂](H₂O)	35.8	0.21	8.7 × 10⁻¹¹	62.3(89.6)	8d
[Co(L¹⁰)₃(NO₃)₂]	35.8	0.21	7.68 ×10⁻⁷	17.7(24.8)	24c
[Co(L¹¹)₃(NO₃)₂]	35.7	0.02	7.01 ×10⁻⁷	11.0(15.8)	24c
[Co(L¹²)](ClO₄)₂	34(1)	0.0	9.90 ×10⁻¹⁰	16.9(24.3)	24d
(PPh₄)₂[Co(NO₃)₄]	12.85	3.60	6.5 × 10⁻¹¹	22.5 (31.5)	10b
(MePh₃P)₂[Co(NO₃)₄]	23.21	0.64	1.9 × 10⁻¹¹	26.6 (37.2)	10b
[Co(tdmmb)(H₂O)₂](BF₄)₂	25.6	-1.0	5.2 × 10⁻⁹	59.2(85.2)	28
[Co(tdmmb)(CN)₂](H₂O)₂	17.3	-0.6	7.4 × 10⁻¹⁰	53.1(76.4)	28
[Co(tdmmb)(NCS)₂]	26.3	-0.0	8.2 × 10⁻⁸	57.1(82.2)	28
[Co(tdmmb)(SPh)₂]	34.5	-1.79	6.5 × 10⁻⁸	68.5(98.6)	28
[Co(L¹³)Br₂]	41(1)	0	1120× 10⁻⁹	4.2 (6.1)	29
[Co(L¹³)I₂]	35(1)	0	1120× 10⁻⁹	4.5 (6.5)	29
[Co(bpy)(NO₃)₂(CH₃CN)]	32.9(2)	0.2(7)	/	39.3 (55.0)	9b
[Co(phen)(NO₃)₂(CH₃CN)]	31.4(2)	0.1(9)	/	32.0 (44.8)	9b
[Co(H₂daps)(MeOH)₂]	43.1(7)	3.3(2)	7.4 × 10⁻⁶	23.9(33.5)	9a
[Co(H₄daps)(NCS)(MeOH)](ClO₄)·(MeOH)	41.5(6)	1.5(4)	5.6 × 10⁻⁶	20.3(28.4)	9a

[Co(H$_4$daps)(NCS)$_2$](MeOH)$_2$	38.8(2)	2.1(7)	4.8×10^{-6}	16.9(23.6)	9a
[Co(napy)$_4$](ClO$_4$)$_2$	25.30	-9.09	3.12×10^{-8}	22.9(32.02)	30
[Co(H$_4$L^{14})(DMF)(H$_2$O)](NO$_3$)$_2$·(DMF)	35.92	1.42	6.5×10^{-6}	17.9(25)	24e
[Co(H$_4$L^{14})(MeOH)(H$_2$O)](NO$_3$)$_2$·(MeOH)	37.23	0.93	3.5×10^{-6}	10.7(15)	24e
[Co(H$_4$L^{14})(DEF)(H$_2$O)](NO$_3$)$_2$	43.76	0.84	1.9×10^{-6}	2.86(4)	24e
[Co(L^{15})(H$_2$O)$_3$]·H$_2$O·H$_2$O	70.41(0)	8.89(7)	/	/	26
[Co(BPA-TPA)](BF$_4$)$_2$	13.1	0.03	3.1×10^{-10}	32.1(45.0)	10a
[Co(BPA-TPA)](ClO$_4$)$_2$·H$_2$O	15.4	0.07	/	/	31
[Co(BPA-TPA)](PF$_6$)$_2$	15.4	0.07	3.73×10^{-6}	4.2 (6.1)	31
[Co(BPA-TPA)](BF$_4$)$_2$	14.6	0.06	5.02×10^{-5}	4.5(6.5)	31

L^9 = 2,13-dimethyl-3,6,9,12-tetraaza-1(2,6)-pyridina-cyclotridecaphane-2,12-diene; L^{10} = 4-tert –butylpyridine; L^{11} = isoquinoline; L^{12} = 3,12-Bis(2-methylpyridine)-3,12,18-triaza-6,9-dioxabicyclo[12.3.1]octadeca-1,14,16-triene; L^{13}= 3,12,18-triaza-6,9-dioxabicyclo[12.3.1]octadeca-1(18),14,16-triene; L^{14} = 2,2′-(pyridine-2,6-diylbis(ethan-1-yl-1-ylidene))bis(N-phenyl-Hydrazinecarboxamide); L^{15} = 8-carboxymethoxy-2-carboxylicquinoline . H$_2$dapb = 2,6-diacetylpyridine bis(benzoylhydrazine); im = imidazole; tdmmb=1,3,10,12-tetramethyl-1,2,11,12-tetraaza[3](2,6)-pyridino[3](2,9)-1,10-phenanthrolinophane-2,10-diene; SPh$^-$=thiophenol anion.; bpy = 2,2'-bipyridine; phen = 1,10-phenanthroline; H$_4$daps = 2,6-bis(1-salicyloylhydrazonoethyl) pyridine; napy = 1,8-naphthyridine; BPA-TPA=2,6-bis(bis(2-pyridylmethyl)amino)methylpyridine；

Table S6. Parameters of one-component Debye's model for Fe(II) compound **3**.

T / K	χ_S / (cm^3 mol^{-1})	χ_T / (cm^3 mol^{-1})	τ /(s)	α	*Residual*
2.0	0.170276E+00	0.812597E+00	0.138217E-03	0.149640E+00	0.100727E-02
2.1	0.159958E+00	0.811411E+00	0.923176E-04	0.149164E+00	0.108164E-02
2.2	0.149135E+00	0.808037E+00	0.615693E-04	0.148912E+00	0.111369E-02
2.3	0.136771E+00	0.805418E+00	0.416051E-04	0.151506E+00	0.113365E-02
2.4	0.119768E+00	0.802649E+00	0.282109E-04	0.158349E+00	0.116981E-02
2.5	0.989768E-01	0.797968E+00	0.192651E-04	0.165411E+00	0.125800E-02
2.6	0.674796E-01	0.792540E+00	0.130096E-04	0.177210E+00	0.110233E-02
2.7	0.235937E-01	0.785186E+00	0.869505E-05	0.187044E+00	0.101843E-02
2.8	0.278751E-04	0.776606E+00	0.616616E-05	0.187684E+00	0.859751E-03